Supplementary Material

Cation exchanges in a fluorescent zinc-based metal-organic framework for cadmium ion detection

Mao-Long Chen[1], Zhen-Li Qi[1], Wan-Ting Jin[2], Zhou Xu[1], Yun-Hui Cheng[1,*], Zhao-Hui Zhou[2,*]

[1]College of Chemistry and Food Engineering, Changsha University of Science & Technology, Changsha, 410114, China; [2]State Key Laboratory of Physical Chemistry of Solid Surfaces, College of Chemistry and Chemical Engineering, Xiamen University, Xiamen, 361005, China.

E-mail: cyh@csust.edu.cn and zhzhou@xmu.edu.cn.

Supplementary Material

Experimental details

1. Chemicals and reagents

All reagents and solvents were of AR grade and used without further purification unless otherwise noted. 2,6-pyridinedicarboxylic acid (99%) was purchased from J&K Scientific Ltd. 1,4-benzenedicarboxylic acid, N,N-Dimethylformamide (DMF), hydrogen peroxide (30%), acetone, $Zn(NO_3)_2{\cdot}6H_2O$ and other metal salt reagents were purchased from Sinopharm Chemical Reagent Co., Ltd. All metal ions standard solutions are prepared by 5% nitric acid. Peach Blossom Rice was purchased from Jinjian Rice Industry (Changsha, China).

2. Instrumentation

IR spectra were recorded as KBr disks and mulls in Nujol with a Nicolet 330 FT-IR spectrophotometer. Thermogravimetric analysis was performed with an SDT-Q600 thermal analyzer under an air flow of 100 $mL{\cdot}min^{-1}$ at a heating rate of 10 $°C{\cdot}min^{-1}$. Powder X-ray diffraction (XRD) data were collected using monochromated Cu Kα radiation on a Phillips X'Pert diffractometer. Phase purity of nano-sized **1** was established by X-ray powder diffraction on a Philips X'Pert diffractometer. The X-ray pattern shows that the positions of the most intense lines remain unchanged relative to the simulated pattern based on the structural data of the complex **1**. Solid-state ^{13}C NMR spectrum was recorded with a Bruker AV 400 NMR spectrometer using cross-polarization, magic angle spinning (13 kHz), and adamantane as the reference. The fluorescence spectra were recorded with an F-7000 FL spectrophotometer. Gas adsorption capacities of **1** were evaluated with a magnetic suspension gravimetric sorption analyzer ISOSORP-HTGRA at 298 K under different pressures of O_2, CH_4, CO_2, N_2, and H_2 respectively. The size and zeta-potentials of the nanomaterial were measured using a Brookhaven NanoBrook 90plus Zeta. The calcination was performed at 5 $°C{\cdot}min^{-1}$ in GSL-1600X-S60 high temperature tube furnace.

*3. Gas adsorptions of **1***

Large quantities of activated **1** have been prepared under heating at 150 °C for one hour and loaded into a magnetic suspension gravimetric sorption analyzer. The gas adsorption data were measured with the change in weight under different pressures of O_2 (CO_2/CH_4/N_2/H_2) inlet conditions at 298 K respectively.

4. Measurement of the HDMA

The HDMA concentration (with one nitrogen) in the solution was determined with a Folinphenol protein quantitative assay. The HDMA solution was diluted to 0.2–0.4 mg/mL with 0.05 mol/L (pH = 8) Na_2HPO_4-NaH_2PO_4 buffer, then 0.5 mL of the diluted sample was drawn into a 10.0 mL glass test tube, 2.5 mL of the alkaline copper reagent was then added, and the mixture was shaken and mixed. After incubation for 10 min,

0.25 mL of Folin-B reagent was added; and the mixture was shaken immediately. The mixture was left to stand at room temperature for 30 min, and the absorbance was measured at 500 nm. The glycine for the standard curve of 0–0.5 mg/mL was linearly fitted, and the nitrogen content of the solution was calculated.

Table S1. Crystal data and structural refinements for **1**.

Empirical formula	$C_{16}H_{21}N_2O_6Zn$
Formula weight	402.72
Temperature/K	193.0
Crystal system	Orthorhombic
Space group	*P* nma
a/Å	18.3597(8)
b/Å	30.884(1)
c/Å	11.3262(4)
Volume/Å^3	6422.2(4)
Z	8
ρ_{cal}cmg/mm^3	0.833
m/mm^{-1}	1.235
F(000)	1672.0
Crystal size/mm^3	0.2 × 0.15 × 0.1
2θ range for data collection	5.724 to 121.396°
Index ranges	-18 ≤ h ≤ 20, -17 ≤ k ≤ 34, -12 ≤ l ≤ 12
Reflections collected	11235
Independent reflections	4910 [*R*(int) = 0.0452]
Data/restraints/parameters	4910/0/230
Goodness-of-fit on *F*2	1.079
Final *R* indexes [$I \geq 2\sigma$ (*I*)]	R_1 = 0.0700, wR_2 = 0.1844
Final *R* indexes [all data]	R_1 = 0.0772, wR_2 = 0.1901
Largest diff. peak/hole / e Å-3	0.77/-0.38

Table S2. Selected bond lengths (Å) for **1**.

Atom-1	Atom-2	Length/Å	Atom-1	Atom-2	Length/Å
Zn1	O2	1.965(3)	C6	C8	1.377(6)
Zn1	O1	1.958(3)	C6	C7	1.368(7)
Zn1	N1	2.063(4)	C6	C5	1.524(6)
Zn1	O3	1.985(3)	C8	C7[2]	1.391(6)
O4	C1	1.248(5)	C1	C2	1.480(6)
O5	C5	1.247(5)	O6	C9	1.235(6)
O2	C5	1.263(6)	C10	C11	1.374(7)
O1	C1	1.281(5)	C10	C9	1.488(7)
N1	C14	1.499(6)	C10	C12	1.382(8)
N1	C13	1.468(7)	C4	C2	1.392(6)
C3	C4[1]	1.404(6)	O3	C9	1.269(6)
C3	C2	1.403(6)	C11	C11[3]	1.40(1)
N2	C15	1.465(7)	C12	C12[3]	1.37(1)
N2	C16	1.477(8)			

[1]-*x*,1 – *y*, -*z*; [2]1 – *x*,1 – *y*, -*z*; [3]+x, ½ – *y*, +*z*

Table S3. Selected bond angles (°) for **1**.

Atom-1	Atom-2	Atom-3	Angle/°	Atom	Atom	Atom	Angle/°
O2	Zn1	N1	109.2(1)	O1	C1	C2	116.4(4)
O2	Zn1	O3	108.3(1)	C6	C7	C8[2]	120.4(4)
O1	Zn1	O2	125.0(1)	C11	C10	C9	120.1(5)
O1	Zn1	N1	103.0(1)	C11	C10	C12	118.2(5)
O1	Zn1	O3	111.1(1)	C12	C10	C9	121.6(5)
O3	Zn1	N1	96.3(2)	C2	C4	C3[1]	120.7(4)
C5	O2	Zn1	109.9(3)	C9	O3	Zn1	110.5(3)
C1	O1	Zn1	118.8(3)	C10	C11	C11[3]	120.6(3)
C14	N1	Zn1	110.7(3)	O5	C5	O2	124.9(4)
C13	N1	Zn1	111.8(3)	O5	C5	C6	118.8(4)
C13	N1	C14	109.8(4)	O2	C5	C6	116.3(4)
C2	C3	C4[1]	120.8(4)	O6	C9	C10	120.0(5)
C15	N2	C16	112.0(4)	O6	C9	O3	123.4(5)
C8	C6	C5	120.4(4)	O3	C9	C10	116.6(5)
C7	C6	C8	119.8(4)	C3	C2	C1	121.0(4)
C7	C6	C5	119.7(4)	C4	C2	C3	118.5(4)
C6	C8	C72	119.8(4)	C4	C2	C1	120.5(4)
O4	C1	O1	124.5(4)	C123	C12	C10	121.2(3)
O4	C1	C2	119.0(4)				

Table S4. Gas adsorption data (mg/g) for CH_4, CO_2, H_2, N_2 and O_2 respectively.

Pressure (bar)	CH_4	CO_2	H_2	N_2	O_2
0.00	0.00	0.00	0.00	0.00	0.00
1.91	3.15	22.43	0.14	1.38	7.80
3.91	4.75	30.19	0.18	2.37	14.85
5.89	6.00	35.13	0.16	3.25	22.47
7.90	6.99	38.42	0.24	3.90	29.59
9.90	7.72	40.94	0.31	4.72	35.11
11.90	8.32	43.31	0.26	5.42	43.10
13.90	8.63	45.13	0.34	5.87	48.77
15.90	8.93	47.09	0.35	6.38	55.82
17.90	9.20	48.11	0.24	6.74	62.87
19.90	9.37	49.63	0.31	7.20	69.97
21.90	9.74	50.50	0.29	7.32	76.03
23.90	9.92	51.86	0.23	7.76	82.47
25.90	10.07	52.91	0.44	8.15	89.21
27.90	9.92	53.70	0.29	8.53	95.63
29.90	10.36	54.53	0.37	8.78	103.07

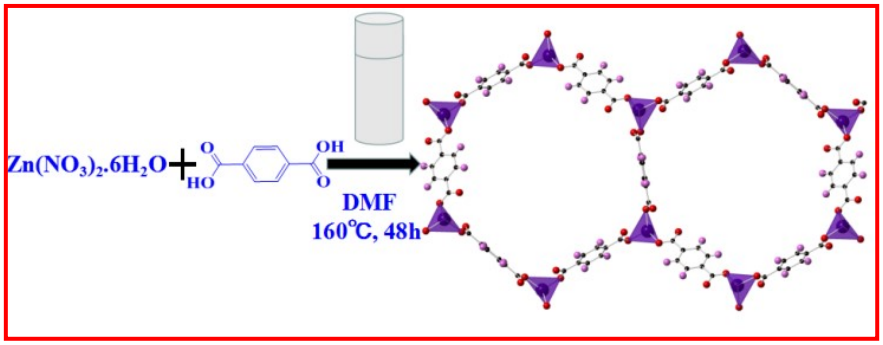

Scheme 1. Schematic diagram of synthetic process.

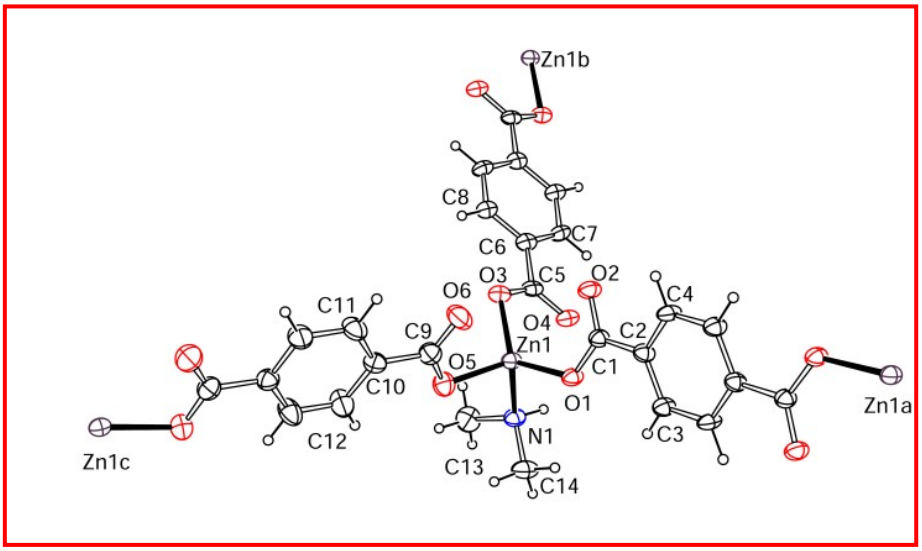

Figure S1. Ortep diagram of 1 at 30% thermal ellipsoids.

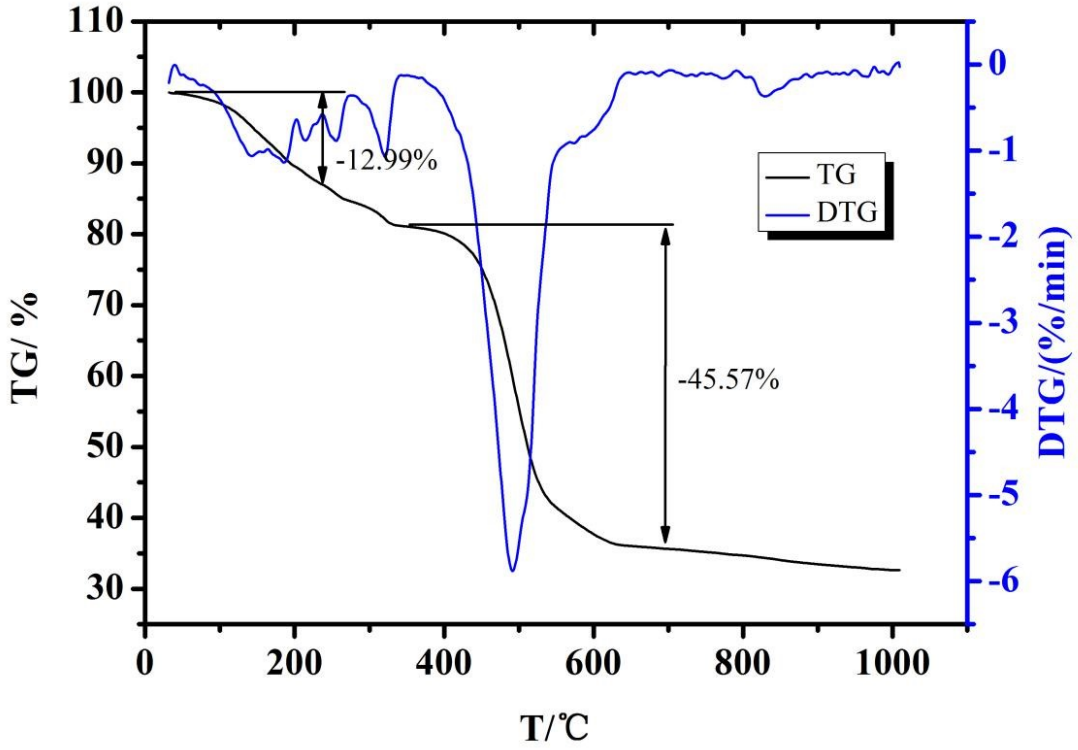

Figure S2. TGA traces of **1** ranging from room temperature to 1000 °C.

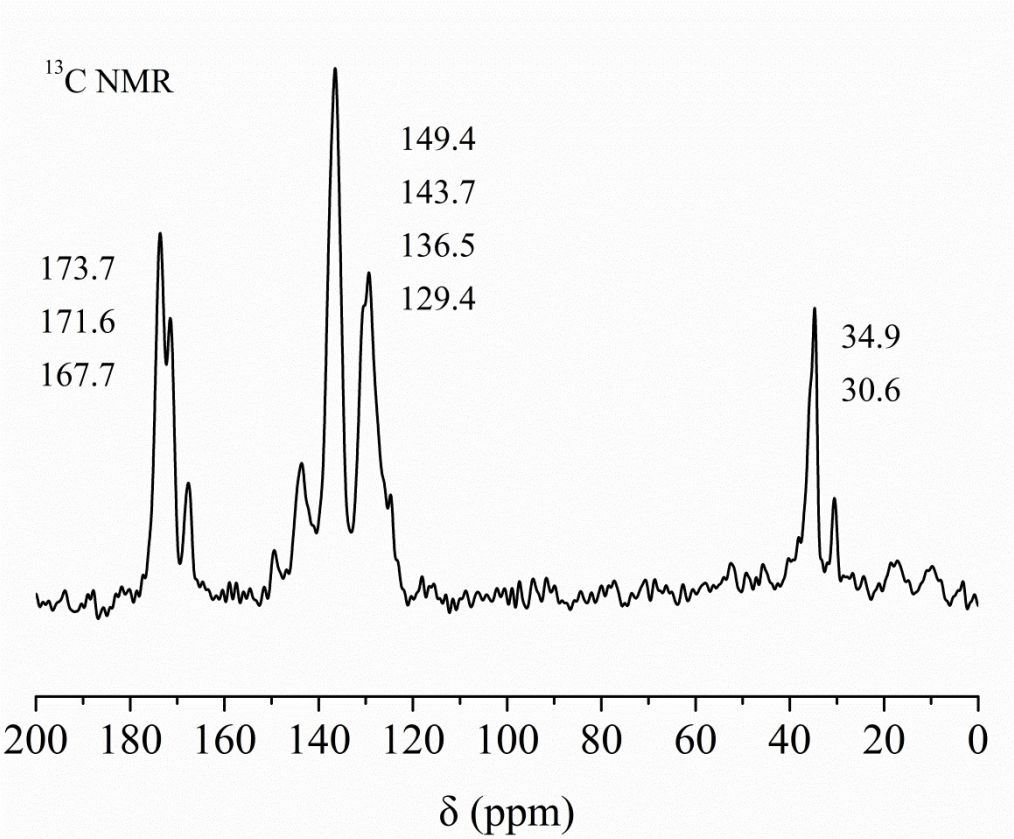

Figure S3. Solid-state ^{13}C NMR spectrum of **1**.

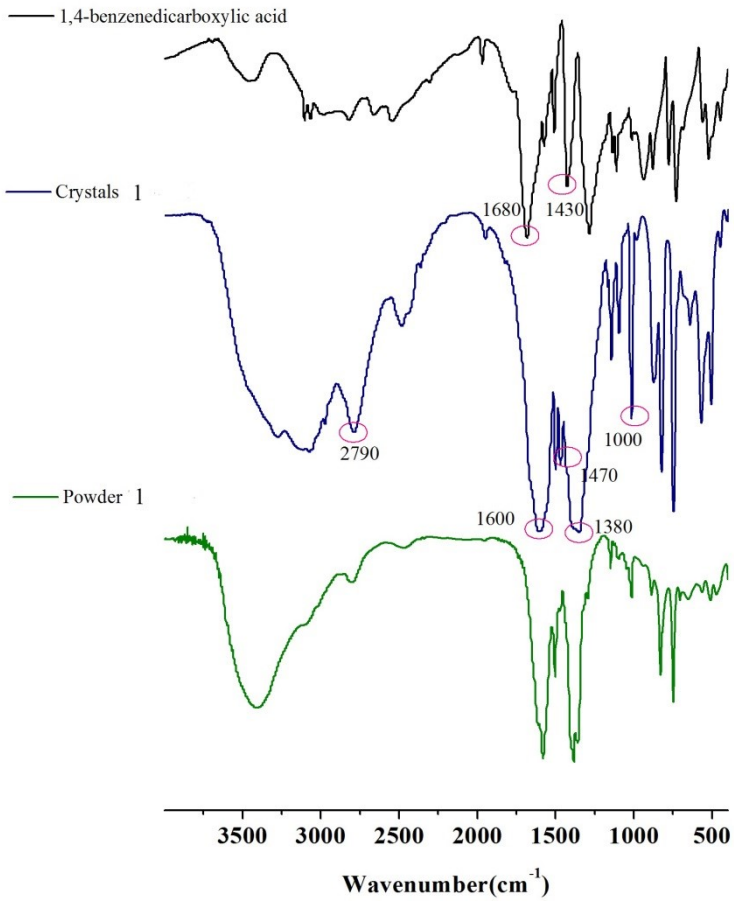

Figure S4. IR spectra of 1,4-benzenedicarboxylic acid and compound **1** and nano-sized **1a**.

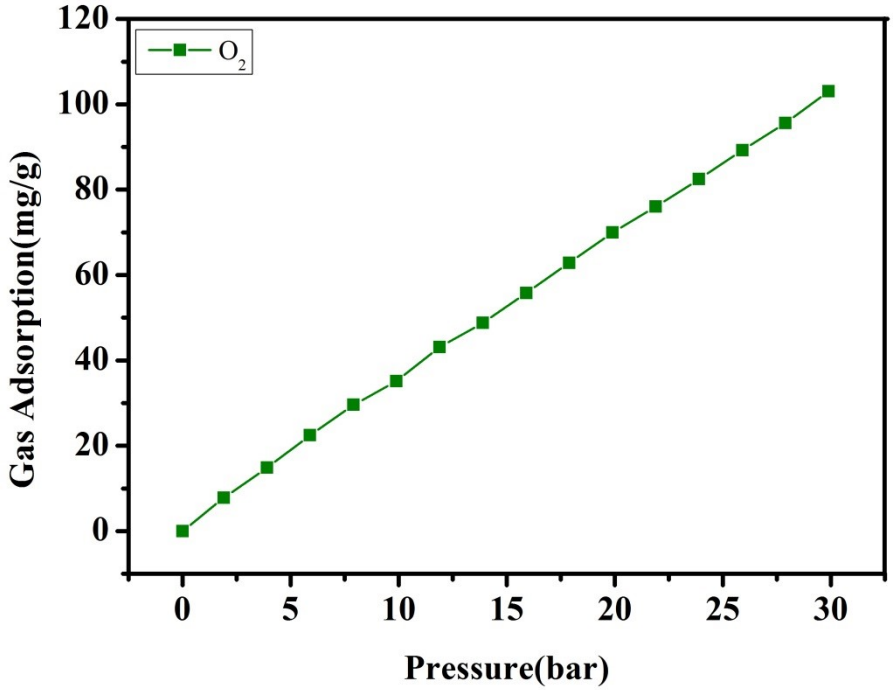

Figure S5. O_2 adsorption isotherms of **1** at 298 K.

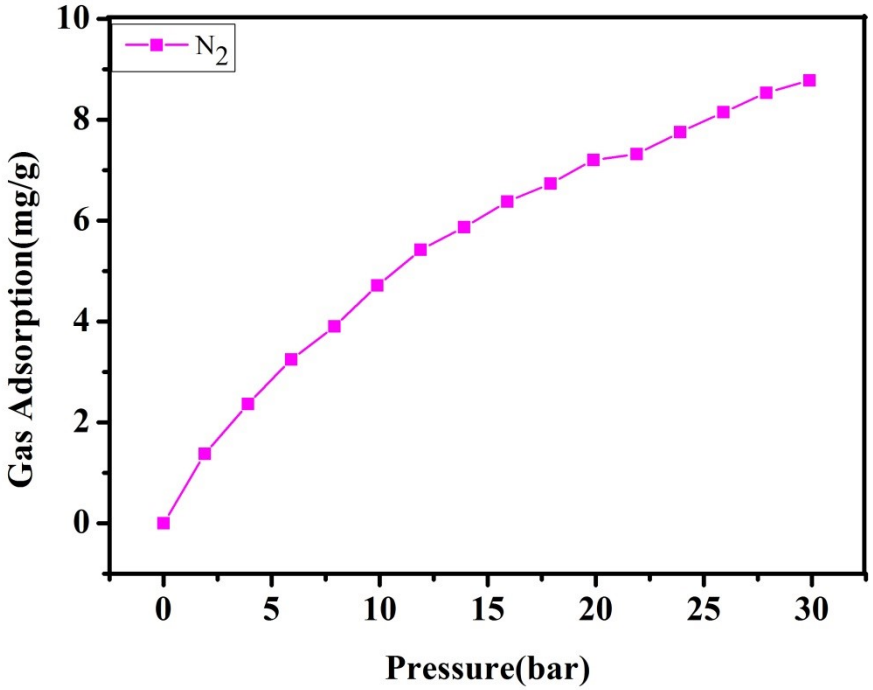

Figure S6. N_2 adsorption isotherms of **1** at 298 K.

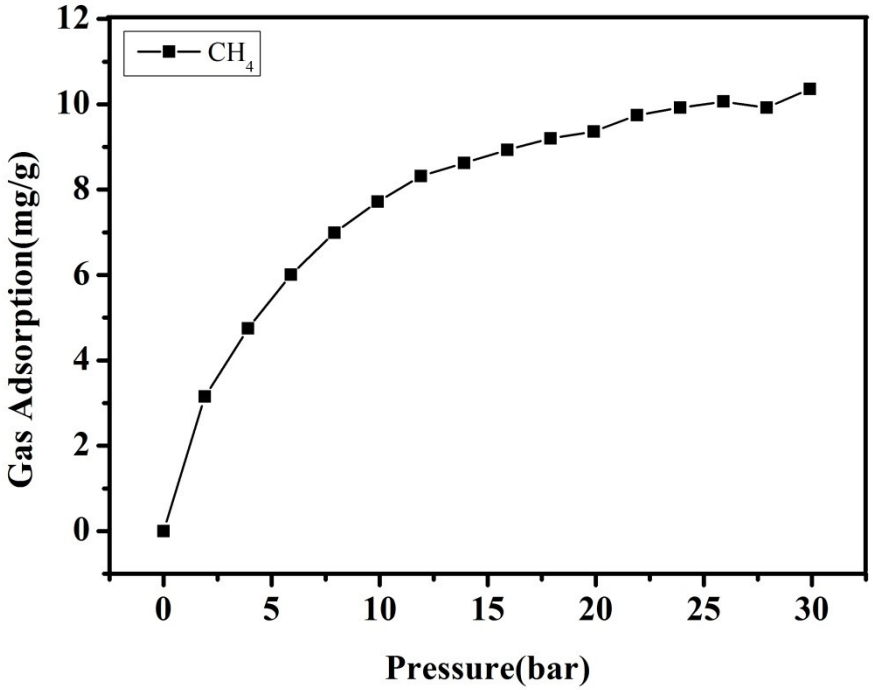

Figure S7. CH_4 adsorption isotherms of **1** at 298 K.

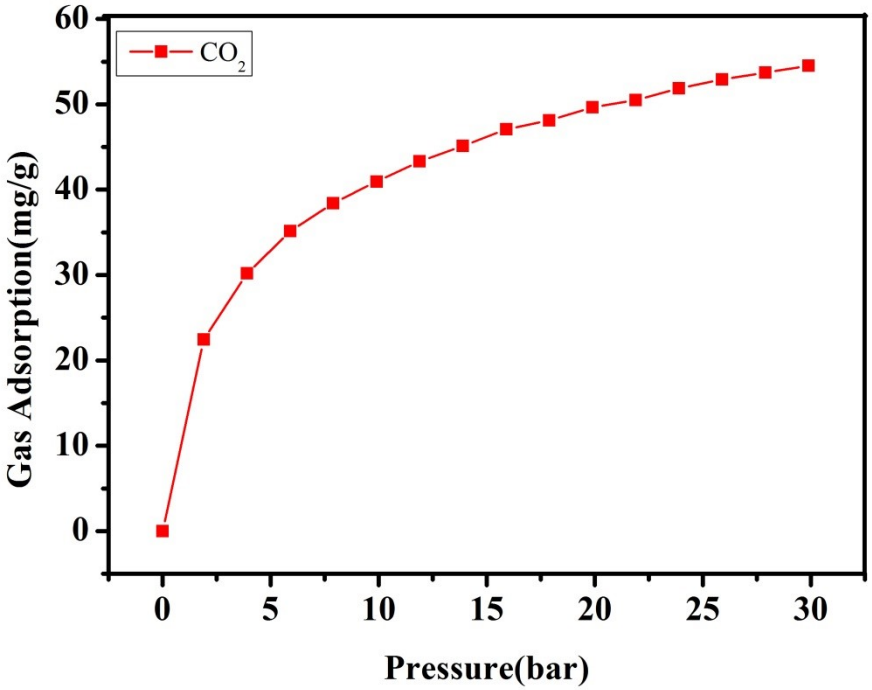

Figure S8. CO_2 adsorption isotherms of **1** at 298 K.

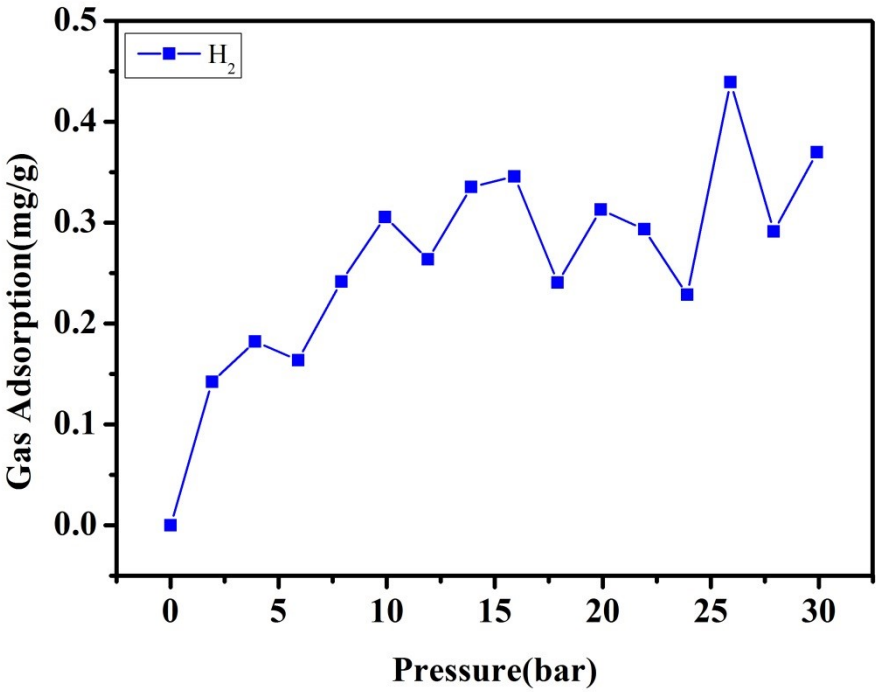

Figure S9. H_2 adsorption isotherms of **1** at 298 K.

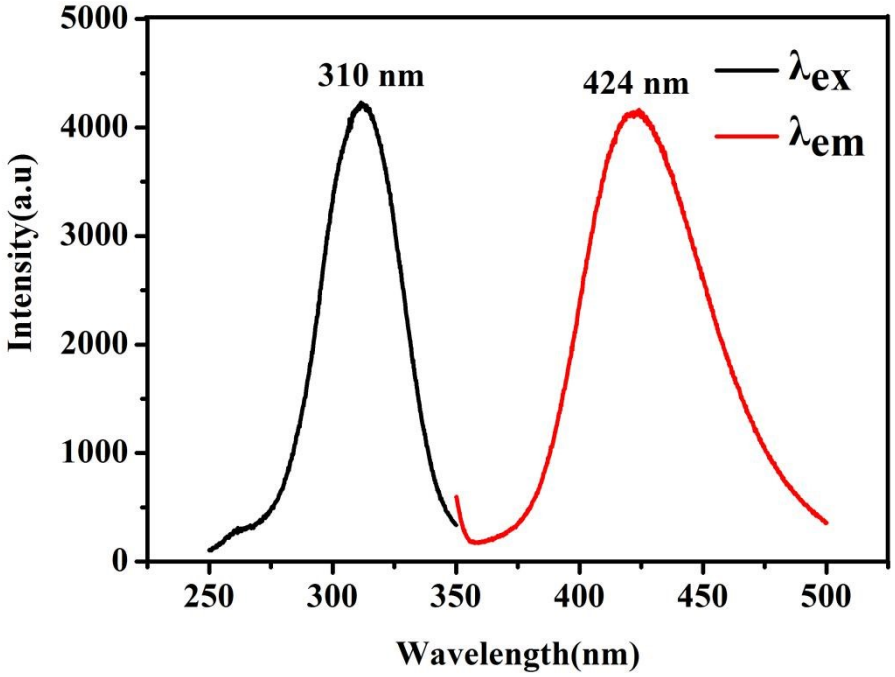

Figure S10. Excitation (black line) and emission (red line) spectra of nano-sized **1**.

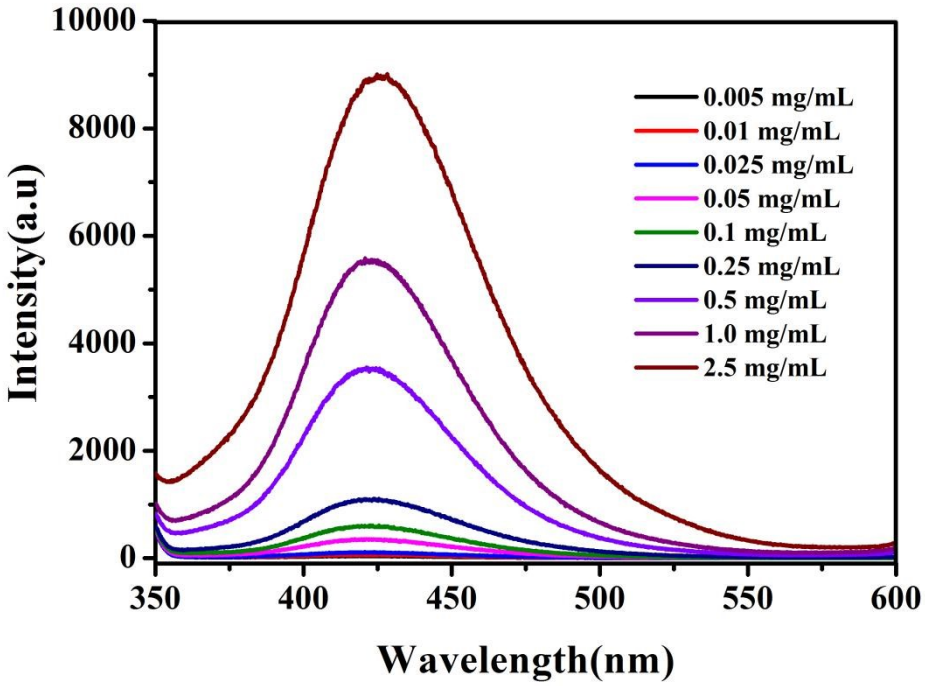

Figure S11. Fluorescence intensities for different concentrations of **1** in aqueous solution (λ_{ex} = 310 nm).

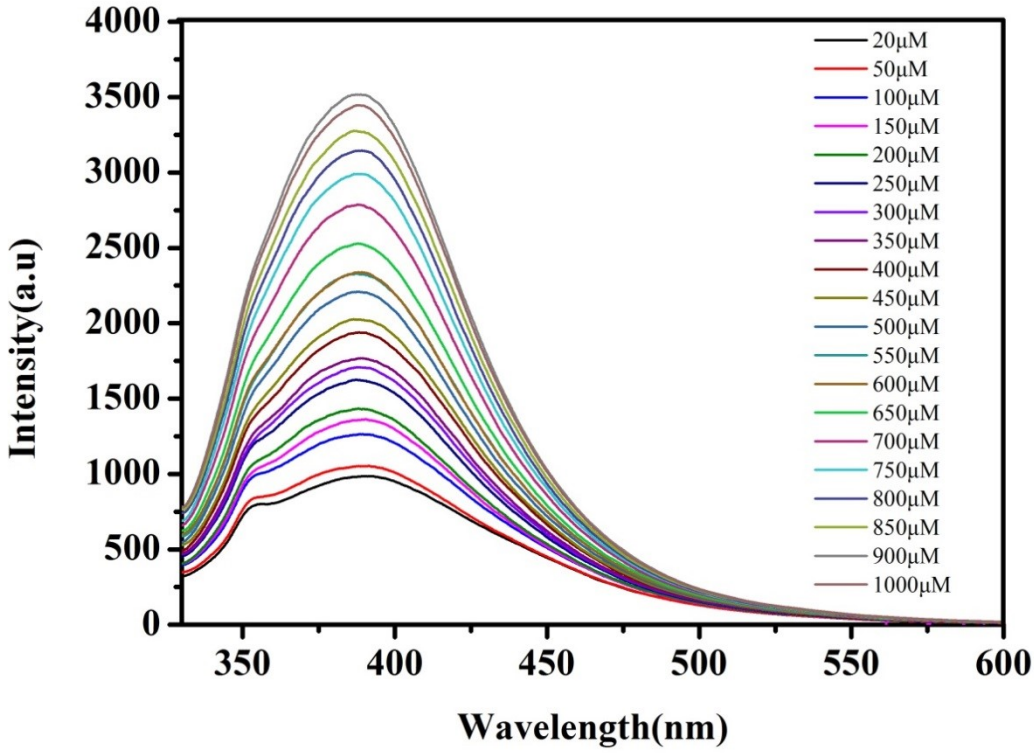

Figure S12. Enhancements in fluorescence emission of sensor **1** in aqueous solution upon continuous additions of 20 ~ 1000 μM of Cd^{2+} .